Phase transitions of nuclear matter beyond mean field theory

Tran Huu Phat,[1] Nguyen Tuan Anh,[2] Nguyen Van Long,[3] and Le Viet Hoa[4]
[1]*Vietnam Atomic Energy Commission, 59 Ly Thuong Kiet, Hanoi, Vietnam and Dong Do University, 8 Nguyen Cong Hoan, Hanoi, Vietnam*
[2]*Institute for Nuclear Science and Technique, 5T-160 Hoang Quoc Viet, Hanoi, Vietnam*
[3]*Gialai Teacher College, 126 Le Thanh Ton, Pleiku, Gialai, Vietnam*
[4]*Hanoi National University of Education, 136 Xuan Thuy, Cau Giay, Hanoi, Vietnam*
(Received 3 July 2007; published 24 October 2007)

The Cornwall-Jackiw-Tomboulis (CJT) effective action approach is applied to study the phase transition of nuclear matter modeled by the four-nucleon interaction. It is shown that in the Hartree-Fock approximation (HFA) a first-order phase transition takes place at low temperature, whereas the phase transition is of second order at higher temperature.

DOI: 10.1103/PhysRevC.76.045202 PACS number(s): 21.65.+f, 05.70.Fh, 11.10.Wx, 21.60.Jz

I. INTRODUCTION

It is known that one of the most important thrusts of modern nuclear physics is the use of high-energy heavy-ion reactions for studying the properties of excited nuclear matter and finding the evidence of nuclear phase transition between different thermodynamical states at finite temperature and density. Such ambitious objectives have attracted intense experimental and theoretical investigations.

Experiments reveal that with increasing excitation energy the behavior of excited nuclei can be described in terms of thermodynamics, and, consequently, in this regime the statistical concepts turn out to be relevant. Numerous experimental analyses indicate that there is dramatic change in the reaction mechanism for excited energy per nucleon in the interval $E^*/A \sim 2$–5 MeV, consistently corresponding to a first- or second-order liquid-gas phase transition of nuclear matter [1–5]. In addition, the critical exponents extracted from experimental data [6,7] are remarkably close to those of liquid-gas system and significantly different from the values derived from the mean-field treatment of this system.

In parallel to experiments, a lot of theoretical articles have been published [8–13], among them, perhaps, the research based on simplified models of strongly interacting nucleons is of great interest for understanding nuclear matter under different conditions. In this respect, this article aims at considering nuclear phase transition in the four-nucleon interaction model developed in Ref. [14] beyond the mean-field approximation. Here we use the CJT effective action formalism and the numerical calculation is carried out in the HFA. In Sec. II we derive the CJT effective potential at finite temperature T and density ρ. Section III is devoted to the numerical computations in HFA. The conclusion and discussion are given in Sec. IV.

II. CJT EFFECTIVE POTENTIAL AT FINITE T AND ρ

Let us begin with the nuclear matter modeled by the Lagrangian density

$$\mathcal{L} = \bar{q}(i\hat{\partial} - M)q + \frac{G_s}{2}(\bar{q}q)^2 - \frac{G_v}{2}(\bar{q}\gamma^\mu q)^2,$$

where M and q are, respectively, the nucleon mass and field operator and G_s, G_v are coupling constants.

Bosonizing

$$\boldsymbol{\sigma} = \frac{g_s}{m_\sigma^2}\bar{q}q, \quad \boldsymbol{\omega}_\mu = \frac{g_v}{m_\omega^2}\bar{q}\gamma_\mu q$$

leads to

$$\mathcal{L} = \bar{q}(i\hat{\partial} - M)q + g_s\bar{q}\boldsymbol{\sigma} q - g_v\bar{q}\gamma^\mu\boldsymbol{\omega}_\mu q - \frac{m_\sigma^2}{2}\boldsymbol{\sigma}^2 + \frac{m_\omega^2}{2}\boldsymbol{\omega}^\mu\boldsymbol{\omega}_\mu, \tag{2.1}$$

in which $G_{s,v} = g_{s,v}^2/m_{\sigma,\omega}^2$, m_σ, and m_ω are, respectively, the masses of scalar and vector mesons. Equation (2.1) clearly resembles the QHD-I Lagrangian of the Walecka model [15] without the kinetic terms for bosons, which describes the symmetric nuclear matter. According to Refs. [14,16,17] the expression for the CJT effective potential reads

$$\begin{aligned} V = {} & \frac{m_\sigma^2}{2}\sigma^2 - \frac{m_\omega^2}{2}\omega^\mu\omega_\mu - i\int\frac{d^4p}{(2\pi)^4}\mathrm{tr}\big[\ln S_0^{-1}(p)S(p) \\ & - S_0^{-1}(p;\sigma,\omega)S(p) + 1\big] + \frac{i}{2}\int\frac{d^4p}{(2\pi)^4}\mathrm{tr}\big[\ln C_0^{-1}C(p) \\ & - C_0^{-1}C(p) + 1\big] + \frac{i}{2}\int\frac{d^4p}{(2\pi)^4}\mathrm{tr}\big[\ln D_0^{\mu\nu-1}D_{\mu\nu}(p) \\ & - D_0^{\mu\nu-1}D_{\mu\nu}(p) + 1\big] - \frac{i}{2}g_s\int\frac{d^4p}{(2\pi)^4}\frac{d^4k}{(2\pi)^4} \\ & \times \mathrm{tr}[S(p)\Gamma(p,k-p)S(k)C(k-p)] + \frac{i}{2}g_v\int\frac{d^4p}{(2\pi)^4} \\ & \times \frac{d^4k}{(2\pi)^4}\mathrm{tr}[\gamma^\mu S(p)\Gamma^\nu(p,k-p)S(k)D_{\mu\nu}(k-p)]. \end{aligned} \tag{2.2}$$

Here

$$\begin{aligned} iS_0^{-1}(k) &= \hat{k} - M, \\ iS_0^{-1}(k;\sigma,\omega) &= iS_0^{-1} + g_s\sigma - g_v\gamma^\mu\omega_\mu, \\ iC_0^{-1} &= -m_\sigma^2, \\ iD_{0\mu\nu}^{-1} &= g_{\mu\nu}m_\omega^2, \end{aligned}$$

S, C, and $D_{\mu\nu}$ are the propagators of nucleon, σ, and ω mesons, respectively;

$$\sigma = \langle \boldsymbol{\sigma} \rangle = \text{const}, \quad \langle \boldsymbol{\omega}_\mu \rangle = \omega \delta_{0\mu} = \text{const}$$

are expectation values of $\boldsymbol{\sigma}$ and $\boldsymbol{\omega}_\mu$ in the ground state of nuclear matter.

The physical solution correspond to

$$\frac{\delta V}{\delta F} = 0, \quad F = \{\sigma, \omega\} \tag{2.3}$$

and

$$\frac{\delta V}{\delta G} = 0, \quad G = \{S, C, D_{\mu\nu}\}. \tag{2.4}$$

Equation (2.3) is the gap equation and (2.4) the Schwinger-Dyson (SD) equation for propagator G.

Inserting Eq. (2.2) into (2.3) yields the gap equations for σ and ω, respectively,

$$\sigma = -\frac{g_s}{m_\sigma^2} \int \frac{d^4p}{(2\pi)^4} \mathrm{tr}[S(p)] = \frac{g_s}{m_\sigma^2} \rho_s, \tag{2.5}$$

$$\omega_\mu = -\frac{g_v}{m_\omega^2} \int \frac{d^4p}{(2\pi)^4} \mathrm{tr}[\gamma_\mu S(p)] = \frac{g_v}{m_\omega^2} \rho, \tag{2.6}$$

where ρ_s and ρ are the scalar and nucleon density, respectively.

The SD equations for propagators S, C, and $D_{\mu\nu}$ are obtained by substituting (2.2) into (2.4) accordingly

$$iS^{-1}(k) = iS_0^{-1}(k) - \Sigma(k), \tag{2.7a}$$

$$\begin{aligned} \Sigma(k) = & -g_s\sigma + g_v\gamma^\mu\omega_\mu \\ & + ig_s \int \frac{d^4p}{(2\pi)^4} [S(p)\Gamma(p, p+k)C(p+k)] \\ & - ig_v \int \frac{d^4p}{(2\pi)^4} [\gamma^\mu S(p)\Gamma^\nu(p, p+k) \\ & \times D_{\mu\nu}(p+k)], \end{aligned} \tag{2.7b}$$

$$iC^{-1}(k) = -m_\sigma^2 - \Pi_\sigma(k) \tag{2.8a}$$

$$\Pi_\sigma(k) = -ig_s \int \frac{d^4p}{(2\pi)^4} \mathrm{tr}[S(p)\Gamma(p, p+k)S(p+k)], \tag{2.8b}$$

$$iD_{\mu\nu}^{-1}(k) = m_\omega^2 g_{\mu\nu} + \Pi_{\omega\mu\nu}(k) \tag{2.9a}$$

$$\begin{aligned} \Pi_{\omega\mu\nu}(k) = & -ig_v \int \frac{d^4p}{(2\pi)^4} \\ & \times \mathrm{tr}[\gamma_\mu S(p)\Gamma_\nu(p, p+k)S(p+k)]. \end{aligned} \tag{2.9b}$$

Σ, Π_σ, and $\Pi_{\mu\nu}$ are self-energies of nucleon, σ, and ω mesons, respectively. Next let us consider the CJT effective potential V in the bare vertex approximation, in which $\Gamma = g_s$ and $\Gamma^\mu = g_v\gamma^\mu$. To this end, let us first expand Σ in terms of its Dirac components

$$\Sigma(k) = \gamma_0\Sigma_0(k) - \vec{\gamma}\vec{k}\Sigma_v(k) - \Sigma_s(k).$$

Due to Eq. (2.7a) the nucleon propagator $S(k)$ is then of the form

$$\begin{aligned} iS^{-1}(k) &= iS_0^{-1}(k) - \Sigma(k) \\ &= \gamma_0 k_0 - \Sigma_0(k) - \vec{\gamma}\vec{k}[1 - \Sigma_v(k)] - [M + \Sigma_s(k)]. \end{aligned}$$

Introducing the effective quantities

$$\begin{aligned} k_0^* &= k_0 - \Sigma_0(k), \\ \vec{k^*} &= \vec{k}[1 - \Sigma_v(k)], \\ M_k^* &= M + \Sigma_s(k) \end{aligned}$$

we arrive at

$$S(k) = (\hat{k}^* + M_k^*)G_k^D, \tag{2.10a}$$

$$\begin{aligned} G_k^D &= -\frac{\pi}{E_k^*}[\delta(k_0^* - E_k^*) + \delta(k_0^* + E_k^*)]n_k^*, \\ n_k^* &= \theta(k_0)n_k^{*-} + \theta(-k_0)n_k^{*+}, \\ n_k^{*\pm} &= \left[e^{(E_k^* \pm \mu^*)/T} + 1\right]^{-1}, \quad \mu^* = \mu - \Sigma_0, \\ E_k^* &= \left[k^{*2} + M_k^{*2}\right]^{1/2}. \end{aligned} \tag{2.10b}$$

In Eq. (2.10a) we retain only the density-dependent part of nucleon propagator, which is dominant at low density [18–20]. Making use of (II.10), respectively, in Eqs. (2.5), (2.6), and (II.7) it is obtained that

$$\sigma = \frac{N_c N_f}{\pi^2} \frac{g_s}{m_\sigma^2} \int_0^\infty p^2 dp \frac{M_p^*}{E_p^*}(n_p^{*-} + n_p^{*+}), \tag{2.11}$$

$$\omega_0 = \frac{N_c N_f}{\pi^2} \frac{g_v}{m_\omega^2} \int_0^\infty p^2 dp \left(n_p^{*-} - n_p^{*+}\right), \tag{2.12}$$

$$\begin{aligned} \Sigma_0(k) = & \frac{N_c N_f}{\pi^2} \frac{g_v^2}{m_\omega^2} \int_0^\infty p^2 dp \left(n_p^{*-} - n_p^{*+}\right) \\ & - \frac{g_s^2}{8\pi^2} \int_0^\infty p^2 dp \int_{-1}^1 d\chi \frac{n_p^{*-} - n_p^{*+}}{M_{p+k}^{\sigma 2}} \\ & + \frac{g_v^2}{4\pi^2} \int_0^\infty p^2 dp \int_{-1}^1 d\chi \frac{n_p^{*-} - n_p^{*+}}{M_{p+k}^{\omega 2}}, \end{aligned} \tag{2.13}$$

$$\begin{aligned} \Sigma_s(k) = & -\frac{N_c N_f}{\pi^2} \frac{g_s^2}{m_\sigma^2} \int_0^\infty p^2 dp \frac{M_p^*}{E_p^*}(n_p^{*-} + n_p^{*+}) \\ & - \frac{g_s^2}{8\pi^2} \int_0^\infty p^2 dp \int_{-1}^1 d\chi \frac{M_p^*}{E_p^* M_{p+k}^{\sigma 2}}(n_p^{*-} + n_p^{*+}) \\ & - \frac{g_v^2}{2\pi^2} \int_0^\infty p^2 dp \int_{-1}^1 d\chi \frac{M_p^*}{E_p^* M_{p+k}^{\omega 2}}(n_p^{*-} + n_p^{*+}), \end{aligned} \tag{2.14}$$

$$\begin{aligned} \Sigma_v(k) = & -\frac{N_c N_f}{\pi^2 k} \frac{g_v^2}{m_\omega^2} \int_0^\infty p^2 dp \int_{-1}^1 d\chi \frac{p^*\chi}{E_p^*}(n_p^{*-} + n_p^{*+}) \\ & + \frac{g_s^2}{8\pi^2 k} \int_0^\infty p^2 dp \int_{-1}^1 d\chi \frac{p^*\chi}{E_p^* M_{p+k}^{\sigma 2}}(n_p^{*-} + n_p^{*+}) \\ & - \frac{g_v^2}{4\pi^2 k} \int_0^\infty p^2 dp \int_{-1}^1 d\chi \frac{p^*\chi}{E_p^* M_{p+k}^{\omega 2}}(n_p^{*-} + n_p^{*+}), \end{aligned} \tag{2.15}$$

where $\chi = \cos(\vec{p^*}, \vec{k^*})$, $M_k^{\sigma 2} = m_\sigma^2 + \Pi_\sigma(k)$, $M_k^{\omega 2} = m_\omega^2 + \Pi_\omega(k)$ and $\Pi^{\mu\nu}(k) = \left(g^{\mu\nu} - \frac{k^\mu k^\nu}{k^2}\right) \Pi_\omega(k)$.

Finally, after some manipulation we are led to

$$
\begin{aligned}
V =& \frac{m_\sigma^2}{2}\sigma^2 - \frac{m_\omega^2}{2}\omega_0^2 + \frac{N_c N_f}{\pi^2}\int_0^\infty p^2 dp\big[T\ln\left(n_p^{*-}n_p^{*+}\right)\\
&- T\ln\left(n_p^- n_p^+\right)\big] - \frac{i}{2}\int\frac{d^4p}{(2\pi)^4}\big[\ln M_p^{\sigma 2} + \ln M_p^{\omega 2}\\
&+ [M_p^\sigma]^{-2} + [M_p^\omega]^{-2}\big] - 2N_c N_f g_s^2\int\frac{d^4p}{(2\pi)^4}\\
&\times\int\frac{d^4k}{(2\pi)^4}\frac{1}{M_{p-k}^{\sigma 2}}\frac{p_0^* k_0^* - \vec{p}^*.\vec{k}^* + M_p^* M_k^*}{\left(p_0^{*2}-E_p^{*2}\right)\left(k_0^{*2}-E_k^{*2}\right)}\\
&- 4i\pi\mathcal{P}N_c N_f g_s^2\int\frac{d^4p}{(2\pi)^4}\int\frac{d^3k}{(2\pi)^4}\left[\frac{p_0^*}{p_0^{*2}-E_p^{*2}}\right.\\
&\left.\times\frac{n_k^{*-}-n_k^{*+}}{M_{p-k}^{\sigma 2}} + \frac{M_p^* M_k^* - \vec{p}^*.\vec{k}^*}{p_0^{*2}-E_p^{*2}}\frac{n_k^{*-}+n_k^{*+}}{E_k^* M_{p-k}^{\sigma 2}}\right]\\
&+ 2\pi^2 N_c N_f g_s^2\int\frac{d^3p}{(2\pi)^4}\int\frac{d^3k}{(2\pi)^4}\int_{-1}^1 d\chi\\
&\times\left[\frac{\left(n_p^{*-}-n_p^{*+}\right)\left(n_k^{*-}-n_k^{*+}\right)}{M_{p-k}^{\sigma 2}} + \frac{M_p^* M_k^* - p^* k^*\chi}{E_p^* E_k^* M_{p-k}^{\sigma 2}}\right.\\
&\left.\times\left(n_p^{*-}+n_p^{*+}\right)\left(n_k^{*-}+n_k^{*+}\right)\right] + 4N_c N_f g_v^2\int\frac{d^4p}{(2\pi)^4}\\
&\times\int\frac{d^4k}{(2\pi)^4}\frac{1}{M_{p-k}^{\omega 2}}\frac{p_0^* k_0^* - \vec{p}^*.\vec{k}^* - 2M_p^* M_k^*}{\left(p_0^{*2}-E_p^{*2}\right)\left(k_0^{*2}-E_k^{*2}\right)}\\
&+ 8i\pi\mathcal{P}N_c N_f g_v^2\int\frac{d^4p}{(2\pi)^4}\int\frac{d^3k}{(2\pi)^4}\left[\frac{p_0^*}{p_0^{*2}-E_p^{*2}}\right.\\
&\left.\times\frac{n_k^{*-}-n_k^{*+}}{M_{p-k}^{\omega 2}} - \frac{2M_p^* M_k^* + \vec{p}^*.\vec{k}^*}{p_0^{*2}-E_p^{*2}}\frac{n_k^{*-}+n_k^{*+}}{E_k^* M_{p-k}^{\omega 2}}\right]\\
&- 4\pi^2 N_c N_f g_v^2\int\frac{d^3p}{(2\pi)^4}\int\frac{d^3k}{(2\pi)^4}\\
&\times\int_{-1}^1 d\chi\left[\frac{\left(n_p^{*-}-n_p^{*+}\right)\left(n_k^{*-}-n_k^{*+}\right)}{M_{p-k}^{\omega 2}}\right.\\
&\left.-\frac{2M_p^* M_k^* + p^* k^*\chi}{E_p^* E_k^* M_{p-k}^{\omega 2}}\left(n_p^{*-}+n_p^{*+}\right)\left(n_k^{*-}+n_k^{*+}\right)\right],
\end{aligned}
\tag{2.16}
$$

and the thermodynamic potential Ω is determined by

$$\Omega = V - V_{\text{vac}}$$

with $V_{\text{vac}} = V(M_{\text{vac}}, \mu = 0, T = 0)$.

In HFA, $\Pi_\sigma = \Pi_\omega = 0$, the expressions for $\Sigma_0(k)$ and $\Sigma_s(k)$ are simplified very much and basing on them we define

$$\mu^* = \mu - \frac{2(2N_c N_f + 1)G_v - G_s}{4\pi^2}\int_0^\infty p^2 dp\left(n_p^{*-} - n_p^{*+}\right), \tag{2.17}$$

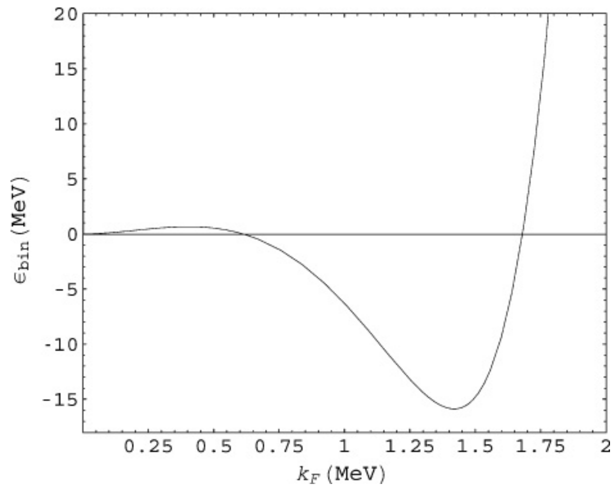

FIG. 1. Density dependence of binding energy per nucleon at saturation point calculated in Hartree-Fock approximation. The coupling constants are independently adjusted to reproduce the binding energy $\epsilon_{\text{bin}} = -15.8771$ MeV at normal density $k_F = 1.4193\ \text{fm}^{-1}$. In this way, $G_s = 161.6/M^2$, $G_v = 1.076G_s$.

$$M^* = M - \frac{(4N_c N_f + 1)G_s + 4G_v}{4\pi^2}\int_0^\infty p^2 dp\frac{M^*}{E_p^*}\left(n_p^{*-} + n_p^{*+}\right). \tag{2.18}$$

Eventually (2.16) becomes

$$
\begin{aligned}
&V(M^*, \mu, T)\\
&= \frac{2N_c N_f (M - M^*)^2}{(4N_c N_f + 1)G_s + 4G_v} - \frac{2N_c N_f(\mu - \mu^*)^2}{2(2N_c N_f + 1)G_v - G_s}\\
&- \frac{N_c N_f}{\pi^2}\int_0^\infty p^2 dp\big[T\ln\left(1 + e^{-(E_p^* - \mu^*)/T}\right)\\
&+ T\ln\left(1 + e^{-(E_p^* + \mu^*)/T}\right)\big].
\end{aligned}
\tag{2.19}
$$

III. NUMERICAL COMPUTATION IN HFA

Starting from Eqs. (2.17), (2.18), and (2.19) let us perform the numerical computations for different cases in HFA.

A. Zero temperature

At $T = 0$ Eqs. (2.17)–(2.19) take simpler forms, which are respectively given by

$$\mu^* = \mu - \frac{2(2N_c N_f + 1)G_v - G_s}{12\pi^2}\left(\mu^{*2} - M^{*2}\right)^{3/2}, \tag{3.1}$$

$$
\begin{aligned}
M^* =& M + \frac{(4N_c N_f + 1)G_s + 4G_v}{8\pi^2}M^*\Big(-\mu^*\sqrt{\mu^{*2} - M^{*2}}\\
&+ M^{*2}\ln|\mu^* + \sqrt{\mu^{*2} - M^{*2}}|\Big),
\end{aligned}
\tag{3.2}
$$

and

$$
\begin{aligned}
&V(M^*, \mu, 0) = -\mu N_c \rho_B\\
&+\frac{2N_c N_f (M - M^*)^2}{(4N_c N_f + 1)G_s + 4G_v} + \frac{2N_c N_f(\mu - \mu^*)^2}{2(2N_c N_f + 1)G_v - G_s}
\end{aligned}
$$

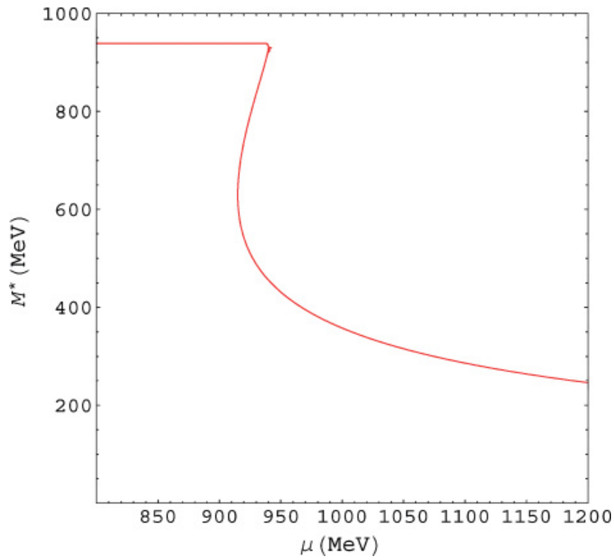

FIG. 2. (Color online) Effective nucleon mass as a function of the chemical potential μ at $T = 0$, illustrating the first-order phase transition. At $\mu_c = 920$ MeV, effective nucleon mass $M_c^* = 760$ MeV. The phase transition is between $\mu = 914$ MeV and $\mu = 940$ MeV.

$$+\frac{N_c N_f}{8\pi^2}\left[\mu^*(2\mu^{*2} - M^{*2})\sqrt{\mu^{*2} - M^{*2}} - M^{*4}\ln\left|\frac{\mu + \sqrt{\mu^{*2} - M^{*2}}}{M^*}\right|\right], \tag{3.3}$$

where ρ_B is the nucleon density,

$$\rho_B = \frac{2}{3\pi^2}k_F^3,$$

with k_F being the Fermi momentum.

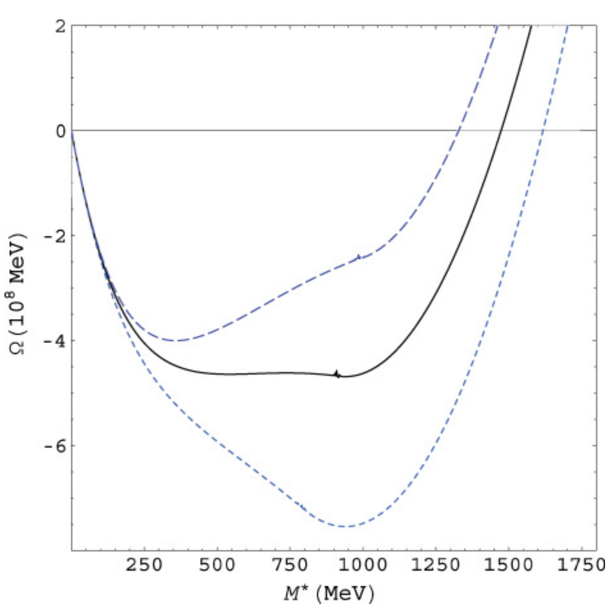

FIG. 3. (Color online) Thermodynamic potential ($\times 10^8$) as a function of the effective nucleon mass M^* at $T = 0$ and $\mu_c =$ 920 MeV (solid line), 800 MeV (dotted line), 1000 MeV (dashed line).

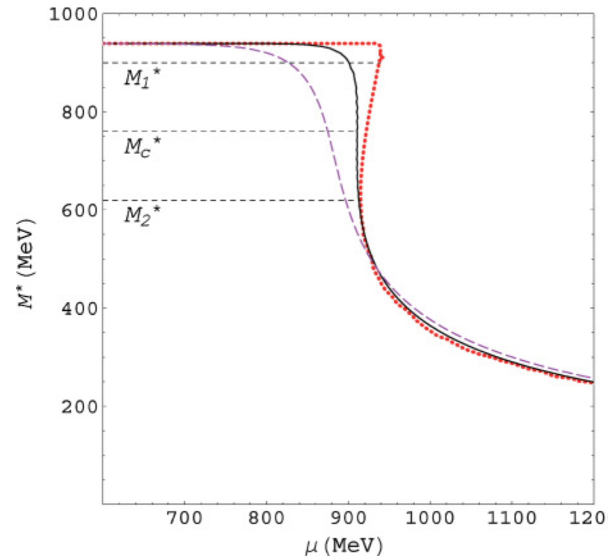

FIG. 4. (Color online) Effective nucleon mass as a function of the chemical potential μ at $T = 1$ MeV (dotted line), $T_c = 20$ MeV (solid line), and $T = 40$ MeV (dashed line).

Now the numerical calculation is readily implemented as follows. At first the masses of nucleon and mesons in vacuum are fixed to be $M = 939$ MeV, $m_\sigma = 550$ MeV, and $m_\omega = 783$ MeV. The next step is to solve numerically Eq. (3.2), the solution$M^*(k_F)$ of which is then substituted into the nuclear binding energy $\epsilon_{\rm bin}$,

$$\epsilon_{\rm bin} = -M + \frac{\varepsilon}{\rho_B},$$

where $\varepsilon = \Omega + \mu\rho_B$ is the energy of system. Two parameters g_s and g_v are adjusted to reproduce the nuclear saturation point as is shown in Fig. 1. We obtain $G_s = 161.6/M^2$ and $G_v = 1.076G_s$.

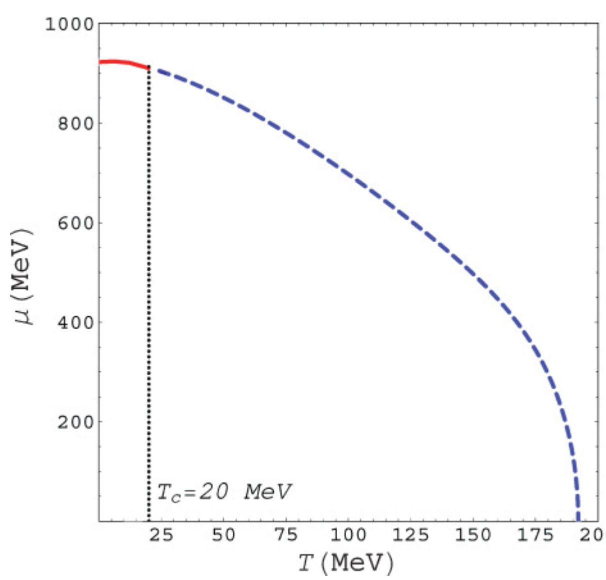

FIG. 5. (Color online) Phase diagram in the T-μ plane. The solid line corresponds to first-order phase transition and the dashed line to second-phase transition.

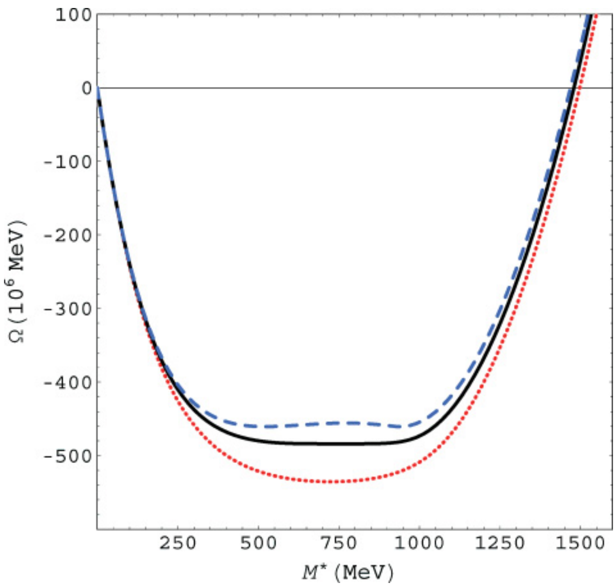

FIG. 6. (Color online) Thermodynamic potential ($\times 10^8$) as a function of the effective nucleon mass M^* at $\{T = 1, \mu = 923\}$ (dashed line), $\{T_c = 20, \mu_c = 910\}$ (solid line), and $\{T = 40, \mu = 880\}$ (dotted line).

By means of Eqs. (3.1) and (3.2) the μ dependence of M^* is depicted in Fig. 2, which gives evidence of first order phase transition at $\mu_c \simeq 920$ MeV.

A better understanding of phase transition is highlighted in Fig. 3, where the M^* dependence of Ω is plotted for several values of μ.

B. Finite temperature and chemical potential

Equations (2.17) and (2.18) determine the μ dependence of M^* at finite temperature. This dependence is given by several graphs in Fig. 4, which correspond to $T = 1$ MeV, 20 MeV, and 40 MeV, respectively.

It is clear that for $T < 20$ MeV a first-order phase transition occurs and begins to smear out at $T = 20$ MeV. For $T > 20$ MeV a second-order phase transition emerges. It is observed that for T raising from low to sufficiently high temperature near $T = 20$ MeV, the pair of points M_1^*, M_2^* will move toward a common point, where the first-order phase transition disappears. This point is close to M_c^*. Therefore, basing on this observation and adopting the definition of critical point proposed in Ref. [21] we are led to the assumption that critical line in the T-μ plane is defined by the equation

$$M^*(\mu_c, T_c) = M_c^*$$

the graph of which is depicted in Fig. 5, where the solid line corresponds to first order phase transition and dashed-line second phase transition.

More detailed information on phase transition is provided in Fig. 6, which shows the M^* dependence of Ω for different temperatures.

IV. CONCLUSION AND DISCUSSION

In the preceding sections the phase transition in nuclear matter was considered in detail beyond the mean-field theory by means of the four-nucleon model. Our major success is that in addition to the familiar first-order phase transition in symmetric nuclear matter, which in our model occurs at low temperature $T \lesssim 20$ MeV, there still exists a second-order phase transition, which comes to emerge for $T > 20$ MeV. It is worth emphasizing that in the mean-field approximation the model reproduces exactly the mean-field results of the Walecka model [15] for bulk nuclear matter. The dramatic change arises when we go beyond this approximation then large fluctuations of order parameters together with their interactions are incorporated into consideration. In our model this nonperturbative effect contributes significantly to critical phenomena. This fact is in contrast to the nonperturbative calculation [22] in the Walecka model, which involves only a first-order phase transition at $T \approx 19$ MeV.

To conclude this article three important remarks are in order.

(i) For describing the bulk nuclear matter properties in the nonperturbative regime the results of both models, four-nucleon and Walecka models, are basically in agreement with each other [14,17,23].

(ii) Lacking chiral symmetry is a serious shortcoming of both models. However, due to Refs. [24,25] the four-nucleon Lagrangian exhibits as the low momentum realization of a nonlinear $SU(2) \times SU(2)$ chiral Lagrangian for strong interactions of pions and nucleons. As a consequence, chiral symmetry can be treated as asymptotic symmetry of nuclear matter described by four-nucleon model. However, it was mentioned [26] that the mean-field QHD-I model is consistent with chiral symmetry that is realized by the nonlinear σ model, but now we are forced to consider the scalar field as an effective degree of freedom and the Lagrangian as a nonrenormalizable effective Lagrangian.

(iii) Starting from the simple model studied earlier a more realistic consideration would be proceeded [27].

ACKNOWLEDGMENTS

This article was financially supported by Vietnam National Foundation for Scientific Research.

[1] V. E. Viola, Nucl. Phys. **A734**, 487 (2004); Phys. Rep. **434**, 1 (2006) and references herein.

[2] V. A. Karnaukhov *et al.*, Phys. Rev. C **67**, 011601(R) (2003); Nucl. Phys. **A734**, 520 (2004) .

[3] B. Borderie *et al.*, Nucl. Phys. **A784**, 595 (2004).

[4] M. D' Agostino *et al.*, Nucl. Phys. **A734**, 512 (2004).

[5] C. B. Das *et al.*, Phys. Rev. C **66**, 044602 (2002).

[6] A. S. Hirsch *et al.*, in *Proceedings of the Corinne II International Workshop on Multi-Particle Correlations and Nuclear Reactions, Nantes, France, September 5–9, 1994*.

[7] D. Kudzia, B. Wilczynska, and H. Wilczynski, Phys. Rev. C **68**, 054903 (2003).
[8] H. Muller and B. D. Serot, Phys. Rev. C **52**, 2072 (1995).
[9] M. Malheiro, A. Delfino, and C. T. Coelho, Phys. Rev. C **58**, 426 (1998).
[10] J. Richert and P. Wagner, Phys. Rep. **350**, 1 (2001) and references herein.
[11] P. Wang, D. B. Leinweber, A. W. Thomas, and A. G. Williams, Phys. Rev. C **70**, 055204 (2004).
[12] A. A. Isayev and J. Yang, Phys. Rev. C **70**, 064310 (2004).
[13] P. Huovinen, Nucl. Phys. **A761**, 296 (2005).
[14] Tran Huu Phat, Nguyen Tuan Anh, and Le Viet Hoa, Nucl. Phys. **A722**, 548c (2003).
[15] B. D. Serot and J. D. Walecka, in *Advances in Nuclear Physics*, edited by J. W. Negele and E. Vogt (Plenum Press, New York, 1986), Vol. 16, p. 1.
[16] J. Cornwall, R. Jackiw, and E. Tomboulis, Phys. Rev. D **10**, 2428 (1974).
[17] Tran Huu Phat and Nguyen Tuan Anh, Nuovo Cimento II A **110**, 475 (1997); **110**, 839 (1997).
[18] M. P. Allendes and B. D. Serot, Phys. Rev. C **45**, 2975 (1992).
[19] G. Krein, M. Nielsen, R. D. Puff, and L. Wilets, Phys. Rev. C **47**, 2485 (1993).
[20] M. Prakash, P. J. Ellis, and J. I. Kapusta, Phys. Rev. C **45**, 2518 (1992).
[21] M. Asakawa and K. Yazaki, Nucl. Phys. **A504**, 668 (1989).
[22] S. Shu and J.-R. Li, Nucl. Phys. **A760**, 369 (2005).
[23] M. Nakano, T. Mitsumori, M. Muraki, K. Koide, H. Kouno, and A. Hasegawa, Phys. Rev. C **49**, 3061 (1994); **49**, 3076 (1994).
[24] S. Weinberg, Nucl. Phys. **13363**, 3 (1991).
[25] G. Gelmini and B. Ritzi, Phys. Lett. **B357**, 431 (1995).
[26] B. D. Serot and J. D. Walecka, Int. J. Mod. Phys. E **6**, 515 (1997).
[27] Tran Huu Phat, Nguyen Tuan Anh, Nguyen Van Long, and Phan Huy Thien (in preparation).